Available online at www.sciencedirect.com

ScienceDirect

IFAC Papers Online CONFERENCE PAPER ARCHIVE

IFAC-PapersOnLine 48-2 (2015) 064–069

Development of a Navigation Algorithm for Autonomous Underwater Vehicles

B. Allotta * **A. Caiti** ** **L. Chisci** *** **R. Costanzi** *
F. Di Corato ** **C. Fantacci** *** **D. Fenucci** ** **E. Meli** *
A. Ridolfi *

* *Department of Industrial Engineering, Florence University, Florence, 50139, Italy, (e-mail: benedetto.allotta@unifi.it)*
** *Centro Piaggio, Pisa University, Pisa, 50122, Italy, (e-mail: andrea.caiti@dsea.unipi.it)*
*** *Department of Information Engineering, Florence University, Florence, 50139, Italy, (e-mail: luigi.chisci@unifi.it)*

Abstract: In this paper, the authors present an underwater navigation system for Autonomous Underwater Vehicles (AUVs) which exploits measurements from an Inertial Measurement Unit (IMU), a Pressure Sensor (PS) for depth and the Global Positioning System (GPS, used during periodic and dedicated resurfacings) and relies on either the Extended Kalman Filter (EKF) or the Unscented Kalman Filter (UKF) for the state estimation. Both (EKF and UKF) navigation algorithms have been validated through experimental navigation data related to some sea tests performed in La Spezia (Italy) with one of Typhoon class vehicles during the NATO CommsNet13 experiment (held in September 2013) and through Ultra-Short BaseLine (USBL) fixes used as a reference (ground truth). Typhoon is an AUV designed by the Department of Industrial Engineering of the Florence University for exploration and surveillance of underwater archaeological sites in the framework of the Italian THESAURUS project and the European ARROWS project. The obtained results have demonstrated the effectiveness of both navigation algorithms and the superiority of the UKF (very suitable for AUV navigation and, up to now, still not used much in this field) without increasing the computational load (affordable for on-line on-board AUV implementation).

Keywords: Autonomous Underwater Vehicles (AUV), Navigation, Ultra-Short BaseLine (USBL), Unscented Kalman Filter (UKF), Extended Kalman Filter (EKF)

1. INTRODUCTION

In this paper, the authors present an navigation system specifically designed for AUVs and its experimental evaluation in typical underwater missions. The developed system exploits inertial sensors (IMU), depth sensors and GPS fixes (during periodic resurfacing) and relies on the Unscented Kalman Filter (UKF) (Julier and Uhlmann (2004), Wan and Merwe (2001), Ristic et al. (2004)) for motion estimation. The proposed navigation system has been experimentally validated through navigation data related to sea tests performed in La Spezia (Italy) with the Typhoon AUV (see Fig. 1, (Allotta et al. (2014a), Allotta et al. (2014b))) in the framework of the Italian THESAURUS project (Allotta and Caiti (2014)) and the European ARROWS project (Allotta (2014)) during the NATO CommsNet13 experiment (Potter (2014)), in September 2013. Typhoon is an AUV designed by the Department of Industrial Engineering of the Florence University for exploration and surveillance of underwater archaeological sites. Currently two versions of the Typhoon AUV have been built, characterized by dfferent sensors and payloads. The vehicles are named TifOne and TifTu respectively. The test campaign described in this paper has been performed using TifTu vehicle equipped with a sensor set including an IMU (with 3D accelerometer, gyroscope and magnetometer), pressure sensor for the depth, GPS and USBL.

Fig. 1. The Typhoon AUV during the sea tests in La Spezia (Italy).

The experimental measurements taken with TifTu AUV include the sensor data concerning the vehicle dynamics (IMU and pressure sensor), global positioning system

10.1016/j.ifacol.2015.06.011

(GPS) fixes obtained through periodic and dedicated vehicle resurfacing (Yun and Bachmann (1999), Marco and Healey (2001)) and global positioning provided by the USBL and obtained thanks to the permanent testbed for underwater networking and communication purposes (LOON - Littoral Ocean Observatory Network) of the Center for Maritime Research and Experimentation (CMRE, formerly NURC). The USBL fixes are not exploited by the new navigation system, being only used as a reference (ground truth) to evaluate the algorithm accuracy.
At this initial stage of the research activity, the experimental underwater test has been performed with the AUV autonomously navigating in dead reckoning along a triangle-shaped path. To effectively evaluate the navigation system performance, the validation has been performed offline, applying the new navigation system to experimental data measured on the vehicle navigating in dead reckoning.
A performance comparison between the proposed UKF-based navigation system and a standard EKF- based system (Allotta et al. (2012)) has been carried out. The comparison allowed the authors to evaluate the accuracy of the proposed navigation approach (very suitable for AUV navigation and, up to now, still not used much in this field) in estimating the vehicle dynamic behaviour without increasing the computational load (affordable for on-line on-board AUV implementation).

2. GENERAL ARCHITECTURE

The typical test architecture is schematized in Fig. 2.

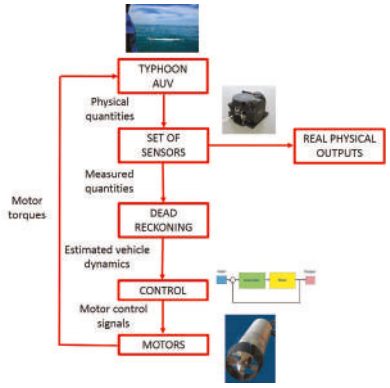

Fig. 2. Online testing of navigation systems.

The Typhoon AUV navigates in dead reckoning using the information coming from the available sensors. The physical quantities characterizing the Typhoon AUV dynamics (orientation, depth and position) are measured by the set of on-board sensors. The measured quantities are then processed in dead reckoning to approximately estimate the vehicle dynamics. Starting from the estimated vehicle dynamics, the control is able to calculate the motor control signals (Allotta et al. (2012)). Finally, the thrusts produced by the motors allow the vehicle to follow the desired dynamics.
The sensor suite provides the real physical outputs to be used to test and compare the different navigation systems (i.e., the EKF-based and UKF-based ones). The preliminary validation and analysis of the navigation system presented by the authors in this work are performed offline. The adopted architecture for offline testing is depicted in Fig. 3.

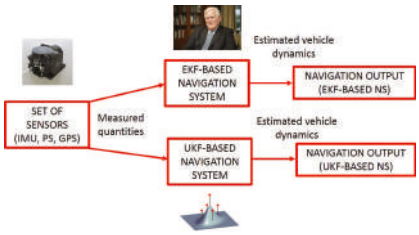

Fig. 3. Offline testing of navigation systems.

The test of the navigation system relies on the data measured by the sensor suite (IMU, pressure sensor and GPS during periodic resurfacings). The measured quantities (orientation, depth and position) are processed by both EKF and UKF algorithms in order to recursively generate estimates of the AUV state. Then, such estimates are compared to the USBL position fixes during the whole mission.

3. THE TYPHOON AUV

In this chapter, the main parts of the Typhoon AUV architecture for the testing of navigation systems are described.

3.1 The vehicle

Typhoon is a middle-sized AUV able to reach a 300 $[m]$ depth. The vehicles can carry suitable payload for the specific underwater mission to perform. Currently, two Typhoons AUVs are fully operative and already performed many missions at sea: the vehicles are called TifOne and TifTu.
TifTu, the AUV exploited during the CommsNet13 sea campaign (Potter (2014)), has a length of 3700 $[mm]$, an external diameter of 350 $[mm]$ and a weight of about 150 $[kg]$ according to the carried payload (the vehicle can be considered an intermediate one compared to the smaller Remus 100 (Packard et al. (2013)) and the bigger Remus 600 (Stokey et al. (2005))). Its autonomy is $8-10\,[h]$ and the maximum reachable longitudinal speed is 6 $[kn]$ (whereas the cruise speed is about 2 $[kn]$). The power needed by the propulsion on-board systems and payloads was approximately known (about 350 $[W]$): considering a mission duration of about $8-10\,[h]$, the needed energy was calculated in about $3-3.5\,[kWh]$. Li-Po (Lithium-Polymer) batteries have been chosen.
In Fig. 4, both the Typhoon CAD design and its final built versions can be seen.

TifTu propulsion system is composed of 6 actuators: two lateral thrusters, two vertical thrusters and two main rear propellers (both working in longitudinal direction). The propulsion system actively controls 5 Degrees Of Freedom (DOFs) of the vehicle (the only one left passive is the roll one).

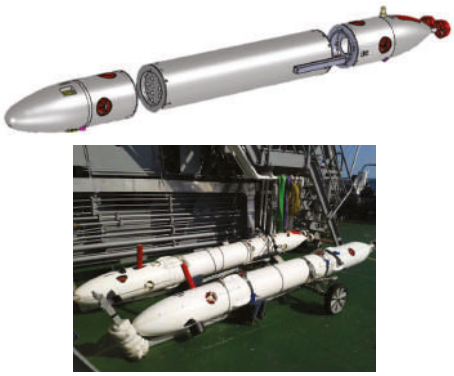

Fig. 4. The Typhoon CAD design and its final built versions on the NATO Alliance RV (CommsNet13).

Vehicle modelling To analyse the motion of the AUV, two different reference frames, shown in Fig. 5, are needed (Fossen (1994)):

- *the body frame*: reference frame with origin O^b placed in the center of mass of the body and axes lined up to the main inertia axes of the body itself.
- *the fixed frame*: inertial reference frame, defined with the origin O^n placed on the surface and axes lined up to the ones of a NED (North-East-Down) frame.

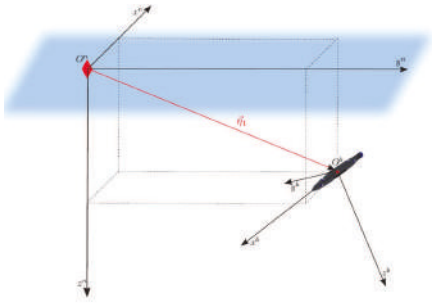

Fig. 5. Body and fixed reference systems.

To describe the motion of the system, the following coordinate vectors have to be introduced:

$$\underline{\eta} = \begin{pmatrix} \underline{\eta}_1 \\ \underline{\eta}_2 \end{pmatrix} = \begin{pmatrix} \underline{O}^b \\ \underline{\Phi} \end{pmatrix}, \quad \underline{\nu} = \begin{pmatrix} \underline{\nu}_1 \\ \underline{\nu}_2 \end{pmatrix} = \begin{pmatrix} \dot{\underline{O}}^b \\ \underline{\omega}^b \end{pmatrix} \tag{1}$$

where $\underline{\eta}$ represents the vector of position $\underline{\eta}_1$ and orientation $\underline{\eta}_2$ (expressed in terms of Euler's angles) in the fixed frame and $\underline{\nu}$ includes the components of linear $\underline{\nu}_1$ and angular $\underline{\nu}_2$ velocities expressed in the body frame. Clearly, the previous physical quantities are linked together by the following kinematic equations:

$$\dot{\underline{\eta}} = J(\underline{\eta})\underline{\nu}, \quad \begin{pmatrix} \dot{\underline{\eta}}_1 \\ \dot{\underline{\eta}}_2 \end{pmatrix} = \begin{bmatrix} J_1(\underline{\eta}_2) & 0_{3x3} \\ 0_{3x3} & J_2(\underline{\eta}_2) \end{bmatrix} \begin{pmatrix} \underline{\nu}_1 \\ \underline{\nu}_2 \end{pmatrix} = \\ = \begin{bmatrix} R_b^n(\underline{\Phi}) & 0_{3x3} \\ 0_{3x3} & T^{-1}(\underline{\Phi}) \end{bmatrix} \begin{pmatrix} \underline{\nu}_1 \\ \underline{\nu}_2 \end{pmatrix} \tag{2}$$

in which R_b^n is the rotation matrix between the body and the fixed reference systems and T is the so called Euler's matrix. On the other hand, the motion of the AUV is governed by the vehicle dynamic equations:

$$M(\underline{\nu})\dot{\underline{\nu}} + C(\underline{\nu})\underline{\nu} + D(\underline{\nu})\underline{\nu} + \underline{g}(\underline{\eta}) = \underline{\tau}(\underline{\nu}, \underline{u}) \tag{3}$$

where M is the mass matrix, C is the centrifugal and Coriolis matrix, D is the drag matrix, $\underline{g}$ is the gravity and buoyancy vector and $\underline{\tau}(\underline{\nu}, \underline{u})$ are the resultant forces and torques acting on the vehicle ($\underline{u}$ are the control signals of the vehicle motors, i. e. the motor rotation speeds). Introducing the state vector $\underline{x} = \begin{pmatrix} \underline{\nu}^T & \underline{\eta}^T \end{pmatrix}^T$, the system equations can be summarized as follows:

$$\dot{\underline{x}} = \underline{F}(\underline{x}, \underline{u}) + \underline{v} = \\ = \begin{pmatrix} M(\underline{\nu})^{-1} \left[\underline{\tau}(\underline{\nu}, \underline{u}) - C(\underline{\nu})\underline{\nu} - D(\underline{\nu})\underline{\nu} - \underline{g}(\underline{\eta}) \right] \\ J(\underline{\eta})\underline{\nu} \end{pmatrix} + \underline{w} \tag{4}$$

where $\underline{w}$ is the process noise.

3.2 The sensors

In the following the set of on-board sensors employed during the navigation by the Typhoon AUV is briefly described:

- *IMU Xsens MTi*: the device consists of a 3D gyroscope, a 3D accelerometer and a 3D magnetometer providing measurements at a maximum working frequency of 100 $[Hz]$. The device estimates the orientation of the vehicle in a 3D space in an accurate way by means of an embedded attitude estimation algorithm;
- *STS DTM depth sensor*: it is a digital pressure sensor used to measure the vehicle depth at a 10 $[Hz]$ working frequency;
- *GPS*: the global positioning system is included into the industrial PC-104. This sensor, working at 1 $[Hz]$, is employed to get suitable fixes only during periodic and dedicated vehicle resurfacing;
- *USBL 18/34 by Evologics*: this sensor is not exploited by the navigation systems and is only used as an external benchmark to evaluate the algorithm accuracy. The sensor works at a maximum working frequency of 0.2 $[Hz]$. Actually, the real working frequency can be quite lower depending on the quality of the acoustic channel.

Sensors modelling Hereafter, the measurement equations modelling the sensor behaviour will be derived by taking into account the main features of the employed sensors and the main noise sources affecting the measurements:

- *vehicle orientation* $\underline{\eta}_2$ provided by the IMU Xsens MTi (including 3D gyroscope, 3D accelerometer and 3D magnetometer) through the attitude estimation filter starting from the following measures:
  - *Vehicle angular velocity* $\underline{\nu}_2$ measured by the 3D gyroscope:
  $$\underline{\nu}_2^{meas} = \underline{\nu}_2 + \underline{\delta}_{\nu 2} \tag{5}$$
  where $\underline{\nu}_2^{meas}$ and $\underline{\nu}_2$ denote the measured and, respectively, true angular velocity and $\underline{\delta}_{\nu 2}$ is the measurement noise;
  - *Vehicle linear acceleration* measured by the 3D accelerometer:
  $$\underline{a}^{meas} = \underline{a} + \underline{\delta}_a \tag{6}$$
  where $\underline{a}^{meas}$ and $\underline{a}$ denote the measured and, respectively, true linear acceleration and $\underline{\delta}_a$ is the measurement noise;

· *Magnetic field* $\underline{M}$ measured by the 3D magnetometer:

$$\underline{M}^{meas} = \underline{M} + \underline{\delta}_M \tag{7}$$

where $\underline{M}^{meas}$ and $\underline{M}$ denote the measured and, respectively, true magnetic field and $\underline{\delta}_M$ is the measurement noise.

By suitably processing the above measurements, the attitude estimation filter is able to estimate the vehicle orientation $\underline{\eta}_2$ that will be used in the subsequent developments of this paper as a virtual measurement $\underline{\eta}_2^{meas}$ modelled as:

$$\underline{\eta}_2^{meas} = \underline{\eta}_2 + \underline{\delta}_{\eta 2} \tag{8}$$

where $\underline{\delta}_{\eta 2}$ is a further measurement noise.

- *vehicle position* η_{1x} and η_{1y} measured by the GPS sensor:

$$\eta_{1x}^{meas} = \eta_{1x} + \delta_x, \quad \eta_{1y}^{meas} = \eta_{1y} + \delta_y \tag{9}$$

where η_{1x}^{meas}, η_{1y}^{meas} and η_{1x}, η_{1y} are the measured and, respectively, true positions and δ_x, δ_y are the measurement noises.

- *vehicle depth* η_{1z} measured by the STS DTM depth sensor:

$$\eta_{1z}^{meas} = \eta_{1z} + \delta_z \tag{10}$$

where η_{1z}^{meas} and η_{1z} are the measured and, respectively, true depth and δ_z is the measurement noise.

All the sensor noise contributions are modelled as zero-mean Gaussian signals.

Introducing the measurement vector $\underline{z} = \left(\underline{\eta}_1^{measT} \ \underline{\eta}_2^{measT} \right)^T$, the measurement equations can be summarized as follows:

$$\underline{z} = \underline{h}(\underline{x}) + \underline{v}, \quad \underline{h}(\underline{x}) = \begin{pmatrix} O_{3x3} & O_{3x3} & I_{3x3} & O_{3x3} \\ O_{3x3} & O_{3x3} & O_{3x3} & I_{3x3} \end{pmatrix} \underline{x},$$
$$\underline{v} = \left(\delta_x \ \delta_y \ \delta_z \ \underline{\delta}_{\eta 2}^T \right)^T. \tag{11}$$

At each time step, the dimension of the measurement vector $\underline{z}$ can be different, depending on the available measurements: the sensors have different working frequencies and may not be always available (see for instance the GPS).

4. EKF-BASED NAVIGATION SYSTEM

The complete system describing the AUV motion

$$\dot{\underline{x}} = \underline{F}(\underline{x}, \underline{u}) + \underline{w}, \quad \underline{z} = \underline{h}(\underline{x}) + \underline{v} \tag{12}$$

has been discretized by the Euler method with sampling interval $\Delta t = 0.01$s taking into account the different working frequencies of the employed sensors:

$$\begin{aligned} \underline{x}_k &= \underline{f}(\underline{x}_{k-1}, \underline{u}_{k-1}) + \underline{w}_{k-1} = \\ &= \underline{x}_{k-1} + \Delta t \, \underline{F}(\underline{x}_{k-1}, \underline{u}_{k-1}) + \underline{w}_{k-1} \\ \underline{z}_k &= \underline{h}(\underline{x}_k) + \underline{v}_k. \end{aligned} \tag{13}$$

The standard navigation system used to estimate the vehicle dynamics is based on the classical EKF estimator (tested offline using the data provided by the Typhoon AUV) (Bar-Shalom et al. (2001), Evensen (2009), Sayed (2009), Allotta et al. (2014b), Allotta et al. (2012)).

5. UKF-BASED NAVIGATION SYSTEM

The UKF is based on the Unscented Transform (UT), a derivative-free technique capable of providing a more accurate statistical characterization of a Random Variable (RV) undergoing a nonlinear transformation (Julier and Uhlmann (2004), Wan and Merwe (2001)). In particular, the UT is a deterministic technique suited to provide mean and covariance of a given RV subjected to a nonlinear function given a minimal set of its samples. The pseudo-code of the UT is reported in Fig. 6. Taking into account mean $\underline{x}$ and associated covariance matrix P of a generic RV as well as a transformation function $g(\cdot)$, the UT proceeds as follows:

- generates $2n_x + 1$ samples $\mathcal{X} \in \mathbb{R}^{n_x \times (2n_x+1)}$, the so called σ-points, starting from the mean $\underline{x}$ with deviation given by the matrix square root Σ of P;
- propagates the σ-points through the transformation function $g(\cdot)$ resulting in $\mathcal{G} \in \mathbb{R}^{n_x \times (2n_x+1)}$;
- calculates the new transformed mean $\underline{\hat{x}}$ and associated covariance matrix P_{yy} as well as the cross-covariance matrix P_{xy} of the initial and transformed σ-points.

Function Unscented Transformation($\underline{y}$, P, g)
▷ Weights are calculated exploiting algorithm in Table 2
1 $\Sigma \longleftarrow \sqrt{P}$
2 $\mathcal{Y} \longleftarrow \left[\underline{y} \dots \underline{y}\right] + \sqrt{c}\left[\underline{0}, \Sigma, -\Sigma\right]$
3 $\mathcal{G} \longleftarrow g(\mathcal{Y})$
4 $\underline{\hat{y}} \longleftarrow \mathcal{G} w_m$
5 $P_{yy} \longleftarrow \mathcal{G} W_c \mathcal{G}^T$
6 $P_{yy} \longleftarrow \mathcal{Y} W_c \mathcal{G}^T$
return $\underline{\hat{y}}$, P_{yy}, P_{xy}
end

Fig. 6. The Unscented Transformation algorithm.

Function Unscented Transformation Weights(α, β, κ)
1 $\lambda \longleftarrow \alpha^2(n_x + \kappa) - n_x$
2 $w_m^{(0)} \longleftarrow \lambda (n_x + \lambda)^{-1}$
3 $w_c^{(0)} \longleftarrow \lambda (n_x + \lambda)^{-1} + (1 - \alpha^2 + \beta)$
4 $w_m^{(1,\dots,2n_x)}, w_c^{(1,\dots,2n_x)} \longleftarrow [2(n_x + \lambda)]^{-1}$
5 $\underline{w}_m = \left[w_m^{(0)}, \dots, w_m^{(2n_x)}\right]^T$,
$\underline{w}_c = \left[w_c^{(0)}, \dots, w_c^{(2n_x)}\right]^T$
6 $W_c \longleftarrow (I - [\underline{w}_m \dots \underline{w}_m]) \times$
$\text{diag}\left(\underline{w}_c^{(0)} \dots \underline{w}_c^{(2n)}\right) \times (I - [\underline{w}_m \dots \underline{w}_m])^T$
7 $c \longleftarrow \alpha^2(n_x + \kappa)$
return c, $\underline{w}_m$, W_c
end

Fig. 7. The Unscented Transformation weights algorithm.

It is worth pointing out that the weights c, w_m and W_c are calculated exploiting the algorithm in Fig. 7, given three parameters α, β and κ. Moment matching properties and performance improvements are discussed in (Julier and Uhlmann (2004), Wan and Merwe (2001)) resorting to specific values of α, β and κ. The UT can be applied in the KF recursion allowing to adopt a nonlinear recursive estimator known as UKF (Julier and Uhlmann (2004)), where also the optimal set of values for the three parameters in case of Gaussian variables is demonstrated. The pseudo-code of the UKF is shown in Fig. 8.

Function Unscented Kalman Filter($\hat{x}_{k-1|k-1}, P_{k-1|k-1}, f(\cdot), h(\cdot)$)

▷ Prediction

1 $\hat{x}_{k|k-1}, P_{k|k-1} \longleftarrow \mathrm{UT}\left(\hat{x}_{k-1|k-1}, P_{k-1|k-1}, f(\cdot)\right)$

2 $P_{k|k-1} \longleftarrow P_{k|k-1} + Q$

▷ Correction

3 $\hat{z}_{k|k-1}, S_k, C_k \longleftarrow \mathrm{UT}\left(\hat{x}_{k|k-1}, P_{k|k-1}, h(\cdot)\right)$

4 $S_k \longleftarrow S_k + R$

5 $\hat{x}_{k|k} \longleftarrow \hat{x}_{k|k-1} + C_k S_k^{-1}\left(z_k - \hat{z}_{k|k-1}\right)$

6 $P_{k|k} \longleftarrow P_{k|k-1} - C_k S_k^{-1} C_k^T$

end

Fig. 8. The Unscented Kalman Filter algorithm.

The main advantages of the UKF approach are the following:

- it does not require the calculation of the Jacobians. Therefore the UKF algorithm is very suitable for highly nonlinear problems and represents a good trade-off between accuracy and numerical efficiency;
- being derivative free, it can cope with functions with jumps and discontinuities;
- it is capable of capturing higher order moments of nonlinear transformations better then the Taylor series based approximation (Julier and Uhlmann (2004)).

6. VALIDATION OF THE NAVIGATION SYSTEM

In this chapter, the navigation system described in section 2 will be validated offline for both classical EKF-based and UKF-based implementations throughout experimental data.

6.1 The experimental campaign

The CommsNet13 experiment took place in September 2013 in the La Spezia Gulf, North Tyrrhenian Sea, with the support of NATO Research Vessel (NRV) Alliance. In the area the CMRE has a permanent testbed for underwater networking and communication purposes (LOON - Littoral Ocean Observatory Network).
One Typhoon class vehicle by UNIFI, in particular TifTu, took part to this experimentation at sea. Throughout the experiments, the TifTu autonomously travelled in dead reckoning and was equipped with the IMU, the pressure sensor for the depth, the GPS sensor (used during the periodic and dedicated resurfacings: one resurfacing every 2.5 minutes) and the USBL unit (used only as ground truth). TifTu travelled along a triangle-shaped path on the LOON area. The reference path for the underwater mission was defined by three waypoints respectively called Janus1, M2 (position of the second one of the four LOON modems) and Typhoon1. The length of the path side was about 190 $[m]$) and the mission was performed at the depth of about 4.5 $[m]$ (see Fig. 9). The TifTu AUV navigated underwater for a total of 1150 $[s]$ at a speed of 0.6 $[m/s]$.

6.2 The mission

In this subsection, the EKF-based and the UKF-based navigation systems will be compared during an underwater mission.

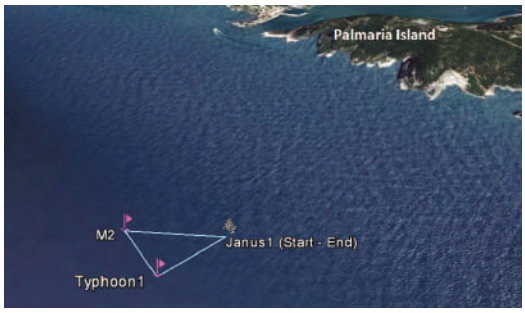

Fig. 9. Layout of the autonomous mission: triangle-shaped path with vertices placed in the waypoints Janus1, M2 and Typhoon1.

Fig. 10 and Fig. 11 show the estimated Cartesian position coordinates η_{1x}^{EKF}, η_{1y}^{EKF} and η_{1x}^{UKF}, η_{1y}^{UKF} provided by both navigation system implementations. The GPS fixes η_{1x}^{GPS}, η_{1y}^{GPS} (during the resurfacings) and the USBL fixes η_{1x}^{USBL}, η_{1y}^{USBL} are also provided for the sake of comparison.

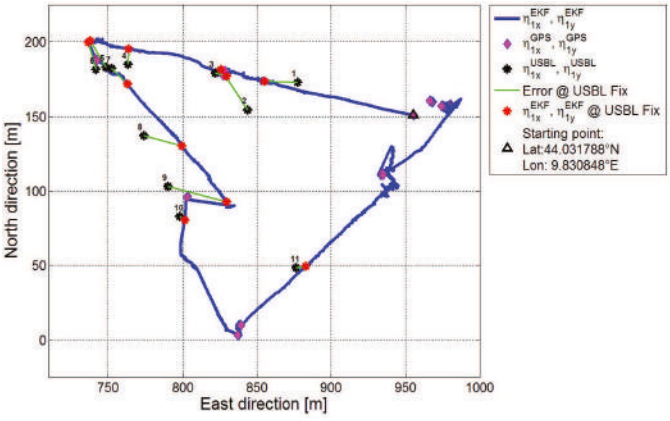

Fig. 10. AUV trajectory estimated by the EKF-based navigation system along with the GPS and USBL fixes (origin coordinates: 44.03042984 ^oN, 9.81893253^oE).

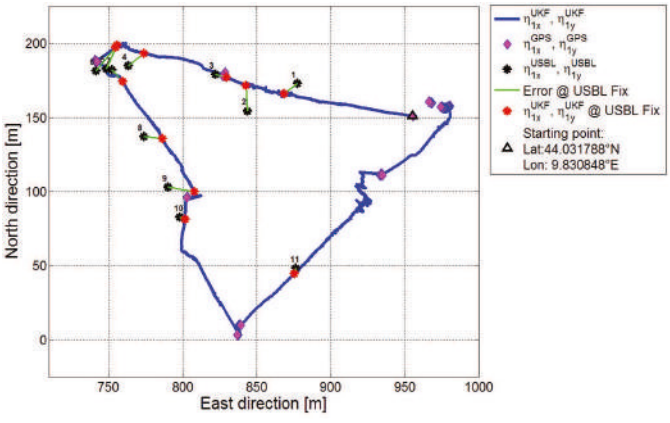

Fig. 11. AUV trajectory estimated by the UKF-based navigation system along with the GPS and USBL fixes (origin coordinates: 44.03042984 ^oN, 9.81893253^oE).

At the same time, Tab. 1 summarizes the USBL fixes η_{1x}^{USBL}, η_{1y}^{USBL} (used as reference), the estimation error

$\left\|\underline{\eta}_1^{EKF} - \underline{\eta}_1^{USBL}\right\|$ affecting $\underline{\eta}_1^{EKF}$ and the estimation error $\left\|\underline{\eta}_1^{UKF} - \underline{\eta}_1^{USBL}\right\|$ affecting $\underline{\eta}_1^{UKF}$.

Table 1. USBL fixes (η_{1x}^{USBL}, η_{1y}^{USBL}) and errors (in $[m]$) affecting $\underline{\eta}_1^{EKF}$ and $\underline{\eta}_1^{UKF}$.

USBL fix	η_{1x}^{USBL}	η_{1y}^{USBL}	EKF Er.	UKF Er.
Fix N^o1	44.031985 ^oN	9.829877 ^oE	22.3	11.1
Fix N^o2	44.031820 ^oN	9.829461 ^oE	32.4	17.0
Fix N^o3	44.032042 ^oN	9.829189 ^oE	7.8	7.7
Fix N^o4	44.032093 ^oN	9.828454 ^oE	10.4	13.6
Fix N^o5	44.032076 ^oN	9.828269 ^oE	20.7	17.3
Fix N^o6	44.032063 ^oN	9.828184 ^oE	18.9	20.8
Fix N^o7	44.032069 ^oN	9.828319 ^oE	14.8	10.6
Fix N^o8	44.031664 ^oN	9.828586 ^oE	26.4	12.4
Fix N^o9	44.031357 ^oN	9.828791 ^oE	40.3	18.1
Fix N^o10	44.031175 ^oN	9.828890 ^oE	4.0	3.8
Fix N^o11	44.030865 ^oN	9.829867 ^oE	6.6	4.0

The classical EKF-based navigation system, representing the standard for the underwater navigation, shows poorer performance compared to the UKF-based one during the whole underwater mission. Therefore, the employment of UKF filter turns out to be quite promising to provide a better accuracy during complex navigation and cooperation tasks and a good trade-off between performance and computational load/implementation complexity.

7. CONCLUSIONS

In this paper, the authors presented an navigation system for AUVs. The system exploits a sensor suite consisting of an Inertial Measurement Unit (IMU), a Pressure Sensor (PS) for the depth and a GPS (used only during periodic and dedicated resurfacings), and relies either on the Extended Kalman Fiter (EKF) or the Unscented Kalman Filter (UKF) for AUV state estimation. Both EKF and UKF navigation algorithms have been experimentally evaluated offline by means of sea navigation tests performed in La Spezia (Italy) with the Typhoon AUV navigating in dead reckoning during the NATO CommsNet13 experiment. Experimental results exhibited a satisfactory localization accuracy for both EKF and UKF, the latter being more accurate than the former.
Some important further developments are scheduled for the near future. First, the UKF-based navigation system will be implemented on-board and tested online on the Typhoon AUV. This way, the performance of the navigation system will be carefully investigated in different critical scenarios. Second, the modelling of the AUV will be further improved and more advanced control techniques (including nonlinear and robust control) will be tested.

ACKNOWLEDGEMENTS

This work has been partially supported by the Italian THESAURUS project (funded by PAR FAS Regione Toscana, Linea di Azione 1.1.a.3) and by the European ARROWS project (this project has received funding from the European Union's Seventh Framework Programme for Research technological development and demonstration, under grant agreement no. 308724). The authors would like to thank the NATO Scientific and Technological Center for Maritime Research and Experimentation (CMRE) (La Spezia, Italy) for providing facilities and support during all the research activity.

REFERENCES

Allotta, B. (2014). http:// www.arrowsproject.eu. *Official Site of the European ARROWS Project*.

Allotta, B., Bartolini, F., Costanzi, R., Monni, N., Pugi, L., and Ridolfi, A. (2014a). Preliminary design and fast prototyping of an autonomous underwater vehicle propulsion system. *Journal of Engineering for the Maritime Environment*, DOI 10.1177/1475090213514040.

Allotta, B. and Caiti, A. (2014). http:// thesaurus.isti.cnr.it. *Official Site of the Italian THESAURUS Project*.

Allotta, B., Costanzi, R., Meli, E., Pugi, L., Ridolfi, A., and Vettori, G. (2014b). Cooperative localization of a team of auvs by a tetrahedral configuration. *Robotics and Autonomous Systems*, 62, 1228–1237.

Allotta, B., Costanzi, R., Monni, N., Pugi, L., Ridolfi, A., and Vettori, G. (2012). Design and simulation of an autonomous underwater vehicle. In *Proceedings of the ECCOMAS 2012 Congress*. Vienna, Austria.

Bar-Shalom, Y., Li, X.R., and Kirubarajan, T. (eds.) (2001). *Estimation with Applications to Tracking and Navigation*. Wiley and Sons, New York, NY, USA.

Evensen, G. (ed.) (2009). *Data Assimilation*. Springer Verlag, Heidelberg, Germany.

Fossen, T. (ed.) (1994). *Guidance and Control of Ocean Vehicles*. John Wiley and Sons, London, UK.

Julier, S. and Uhlmann, J. (2004). Unscented filtering and nonlinear estimaion. *Proc. of the IEEE*, 92, 401–422.

Marco, D. and Healey, A. (2001). Command, control, and navigation experimental results with the nps aries auv. *IEEE Journal of Oceanic Engineering*, 26, 466–476.

Packard, G., Kukulya, A., Austin, T., Dennett, M., Littlefield, R., Packard, G., Purcell, M., Stokey, R., and Skomal, G. (2013). Continuous autonomous tracking and imaging of white sharks and basking sharks using a remus-100 auv. In *Proceedings of the IEEE OCEANS 2013*. San Diego, CA, USA.

Potter, J.R. (2014). http:// fp7-sunrise.eu/ index.php/ news/19-commsnet1. *Official Site of the NATO CommsNet13 Experiment*.

Ristic, B., Arulampalam, S., and Gordon, N. (eds.) (2004). *Beyond the Kalman Filter*. Artech House Publishers, Boston, MA, USA.

Sayed, A.H. (ed.) (2009). *Adaptive Filters*. Wiley and Sons, Hoboken, NJ, USA.

Stokey, R., Roup, A., von Alt, C., Allen, B., Forrester, N., Austin, T., Goldsborough, R., Purcell, M., Jaffre, F., Packard, G., and Kukulya, A. (2005). Development of the remus 600 autonomous underwater vehicle. In *Proc. of the IEEE OCEANS 2005*. Washington D.C.,USA.

Wan, E.A. and Merwe, R. (eds.) (2001). *The Unscented Kalman Flter*. S. Haykin Edition, New York, NY, USA.

Yun, X. and Bachmann, E. (1999). Testing and evaluation of an integrated gps/ins system for small auv navigation. *IEEE Journal of Oceanic Engineering*, 24, 396–404.